ISSN 0031-918X, Physics of Metals and Metallography, 2019, Vol. 120, No. 10, pp. 989–994. © Pleiades Publishing, Ltd., 2019.
Russian Text © The Author(s), 2019, published in Fizika Metallov i Metallovedenie, 2019, Vol. 120, No. 10, pp. 1083–1088.

STRENGTH AND PLASTICITY

Effect of The Processes of Self-Tempering and Tempering on The Mechanical Characteristics and the Character of Fracture of Low-Carbon Martenstic Steel Quenched in Air

R. A. Vorobev[a], *, V. N. Dubinskii[a], and V. V. Evstifeeva[b]

[a] *Alekseev NGTU, Nizhny Novgorod, 603950 Russia*

[b] *SC CRI Burevestnik, Nizhny Novgorod, 603950 Russia*

**e-mail: linuxjuicy@gmail.com*

Received February 2, 2019; revised March 12, 2019; accepted March 20, 2019

Abstract—The influence of the processes of self-tempering and tempering on the mechanical characteristics and structure of low-carbon martensitic steel after air-quenching has been considered in this work. The processes of martensite decomposition (self-tempering) that started upon cooling continue in the steel in the course of subsequent tempering at 200, 300, 400, and 500°C with the formation of a ferrite–carbide mixture of different degrees of dispersion. Upon tempering at temperatures of 200–400°C, a monotonic increase is noted in the yield stress by 11%; the tempering at 500°C leads to a 3% reduction in the yield stress. The character of the fracture of the samples was studied using scanning electron microscopy; this study has confirmed the phenomenon of temper brittleness in the steel at temperatures of 300 and 500°C, which is in good agreement with the results of mechanical tests.

Keywords: heat treatment, low-carbon martensitic steels, mechanical tests, microstructure, structure of fracture surfaces

DOI: 10.1134/S0031918X19100132

INTRODUCTION

A new class of structural low-carbon martensitic steels (LCMSs) containing less than 0.2% C was developed in the 1980s, in which the lath structure of the martensite ensures a high mobility of dislocations and their high density (10^{10}–10^{12} cm^{-2}). The LCMSs have a better complex of mechanical properties and a better technological effectiveness in comparison with the traditional structural steels with a strength of 800–1400 MPa [1–3]. They find increasingly wider use in general and special engineering for the manufacture of products in the oil-producing industry, load-lifting mechanisms, building, and special equipment operating under heavy conditions, in the complex-stressed states under static, dynamic, and cyclic loads, at low (down to –70°C) and enhanced (up to 500°C) temperatures. The possibility of quenching in air of products made from these steels is among the technological advantages of the LCMSs.

In this work we examined steel 07Kh3GNMYuA, which belongs to the class of purely martensitic steels: no bainite is formed in it upon quenching in air, unlike most other LCMSs. However, the high value of the martensitic point should ensure a significant development of self-tempering processes upon quenching.

The aim of this work is to study the processes of structure formation that occur during self-tempering and tempering (at different temperatures) and their impact on the mechanical characteristics and character of fracture of the 07Kh3GNMYuA steel after a strengthening heat treatment (HT).

EXPERIMENTAL

The microstructure formation and its impact on the complex of mechanical properties was studied using samples of steel 07Kh3GNMYuA after various regimes of heat treatment: quenching from 910°C in air; tempering at T_{temp} = 200, 300, 400, 500°C for 3 hours; cooling in the same way as upon quenching, i.e., in air. The chemical composition of the steel was determined using a Foundry Master spectroanalyzer (OXFORD INSRUMENTS). The content of the main chemical elements (%) is as follows: Fe = 94.20, C = 0.064, Si = 0.271, Mn = 0.914, P = 0.003, S = 0.011, Cr = 2.98, Mo = 0.23, Ni = 1.00, Al = 0.021, Co = 0.021, Cu = 0.21, V = 0.009, W = 0.015.

The hardness measurements were carried out using a Rockwell 574 hardness meter (GOST 9013–59).

The impact toughness was determined on Ménager samples (10 × 10 × 55 mm) with a U-shaped notch

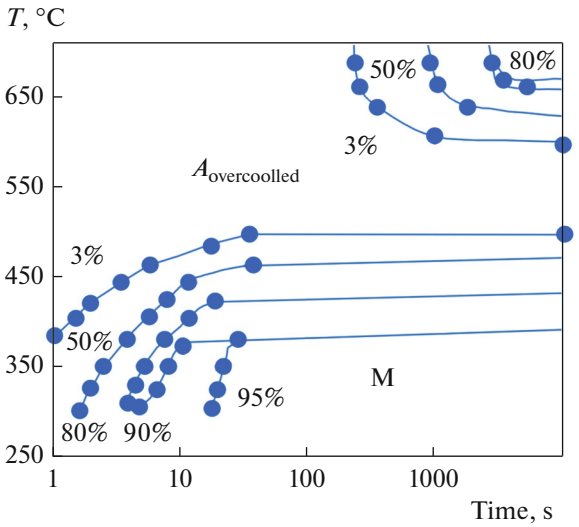

Fig. 1. Diagram of the isothermal transformation of the overcooled austenite of steel 07Kh3GNMYuA.

using a PH-300 impact machine (Walter + Bai AG) with an impact energy of 300 J (GOST 9454–78).

The mechanical characteristics were measured using an "Inspekt 100 table" testing machine.

The photographs of the microstructures and fractures were obtained by the SEM method using a VEGA 3 XMH microscope (TESCAN) with a thermoemission cathode made from lanthanum hexaboride (LaB_6). The images were recorded using a secondary-electron detector under the following conditions: acceleration voltage 20 kV; the intensity of the electron beam 10–13 A; the working distance 6–22 mm.

RESULTS

The diagram of the isothermal decomposition of the austenite of the 07Kh3GNMYuA steel is presented in Fig. 1. The high stability of the austenite of the 07KhGNMYuA steel in the range of the pearlite transformation, the lack of upper bainite, the high temperature of the martensitic transformation M_{mt} (390°C), which provides self-tempering during cooling, leads to the formation of a tempered low-carbon martensite even upon slow cooling. Such a structure and the weak dependence of the viscosity on the grain size guarantee a favorable combination of the characteristics of strength, plasticity, and toughness [4, 5]. The development of the self-tempering results in the formation of a packet "structureless" martensite alternating with regions of ferrite (Fig. 2a).

After quenching in air in the investigated range of temperatures of tempering (200–500°C), structures of various phase compositions are formed in the steel 07Kh3GNMYuA. These structures differ in the type and ratio of phases, their dispersion and their location, which results in different combinations of standard mechanical characteristics of the steel determined in the usual work practice. The mechanical characteristics of the steel 07Kh3GNMYuA after heat treatment are presented in Table 1.

As a result of processes of self-tempering upon cooling of the 07Kh3GNMYuA steel in air, the martensite laths begin to be fragmented (see Fig. 2a), and the martensite becomes "structureless." The presence of tempered martensite in the steel structure indicates that already upon cooling in air there occur in the resulting martensite a redistribution of carbon atoms in the solid solution and their movement to dislocations, as well as the martensite decomposition with the formation of carbon-enriched regions (segregates), and then of carbide precipitates [6, 7].

The beginning processes of martensite decomposition during air-quenching continue upon subsequent temperings at 200, 300, 400, and 500°C.

The reduction of the carbon supersaturation of the solid solution in the temperature range of 200–400°C and the occurring processes of first-order recovery result in a partial relaxation of internal stresses, which is likely to result in an increase of the impact toughness relative to its value in the quenched condition. However, after tempering, elastic microstresses arise at coherent interphase boundaries, because of an increased resistance to the movement of the dislocations due to their pinning by carbon segregates [8]; as a result, the hardness is retained at a level of 30 HRC, and the yield stress is increased.

In the microstructure of the steel 07Kh3GNMYuA, upon an increase in the recovery temperature an intensification occurs of the martensite fragmentation, both take place a decomposition of the solid solution and a precipitation of a carbide phase of glob-

Table 1. Mechanical properties of steel 07Kh3GNMYuA

Regime of heat treatment	*KCU*, J/cm^2	$\sigma_{0.2}$, MPa	σ_u, MPa	Ψ, %	δ, %	HRC
Quenching at 910°C in air	129	747	1019	65.8	14.8	31
Quenching at 910°C in air, tempering at 200°C	141	782	1021	66.2	15.0	30
Quenching at 910°C in air, tempering at 300°C	133	822	1016	67.0	14.4	30
Quenching at 910°C in air, tempering at 400°C	142	829	995	65.9	15.6	30
Quenching at 910°C in air, tempering at 500°C	111	805	1001	65.8	16.0	26

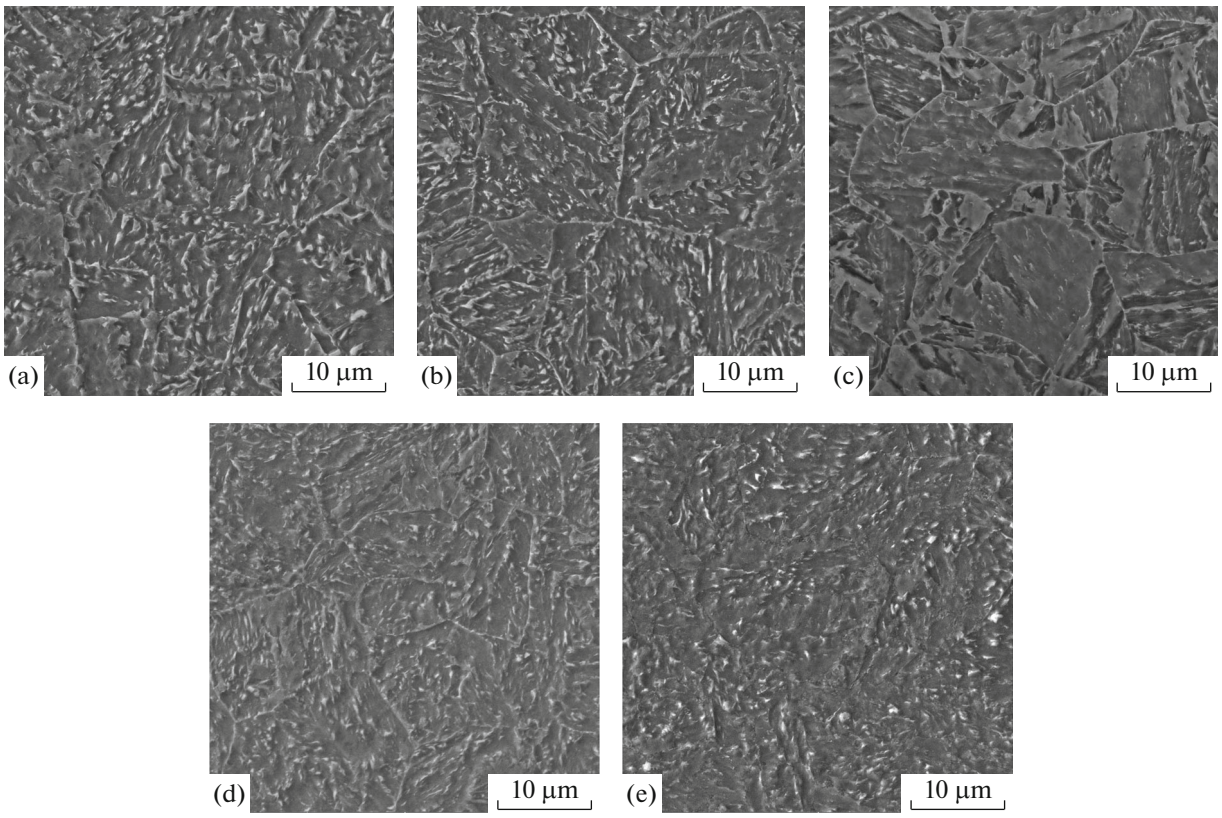

Fig. 2. Structure of steel 07Kh3GNMYuA: (a) after cooling in air; (b) after tempering at 200°C; (c) after tempering at 300°C; (d) after tempering at 400°C; and (e) after tempering at 500°C.

ular morphology, which follows the orientation of the former lath packets (Figs. 2b, 2c, 2d). Correspondingly, as the recovery temperature increases from 200 to 400°C, the resistance to plastic deformation increases: a monotonic increase is noted in the yield stress $\sigma_{0.2}$ of air-quenched samples by about 11% (from 747 to 829 MPa). As the tempering temperature is increased to 500°C, the yield stress decreases by 3% ($\sigma_{0.2} = 805$ MPa). The ultimate strength σ_u in the entire range of tempering temperatures 200–500°C decreases, though only slightly, from 1021 to 1001 MPa (Fig. 3).

After tempering at 500°C, the reduction of the yield stress of the steel occurs via the coagulation of the carbide phase and reduction of its dispersion. The lathlike morphology of the carbide phase is not revealed visually; the structure represents a highly dispersed ferrite–carbide mixture (Fig. 2e).

The plasticity characteristics of the 07Kh3GNMYuA steel vary insignificantly depending on the tempering temperature. The change in the relative reduction ψ (from 65.8 to 67.0%) was within the measurement error ($\varepsilon < 1\%$).

The relative elongation δ proved to be slightly more sensitive to the degree of tempering (Fig. 4): upon the steel tempering at 200, 400, and 500°C, the elongation δ increases from 14.8 to 15.0, 15.6, and 16.0%, respectively (with ε not exceeding 1%). After tempering at 300°C, there is a dip in the plot; the relative elongation decreases to 14.4%; no consistent increase in plasticity is observed with increasing tempering temperature.

Anomalous dips in the curves of tempering are observed at 300 and 500°C (temper brittleness) during tests for the impact toughness of samples with a

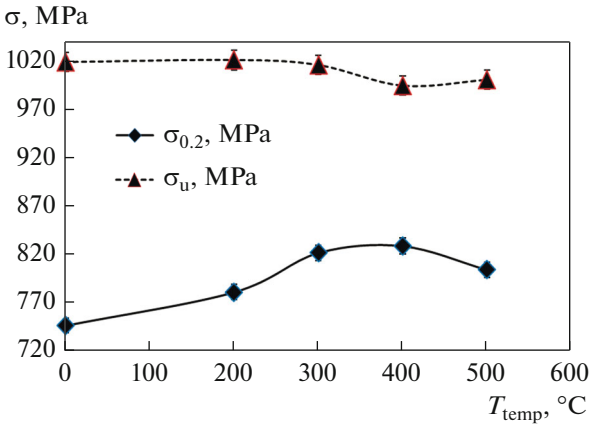

Fig. 3. Dependence of the strength characteristics of the 07Kh3GNMYuA steel quenched in air on the tempering temperature.

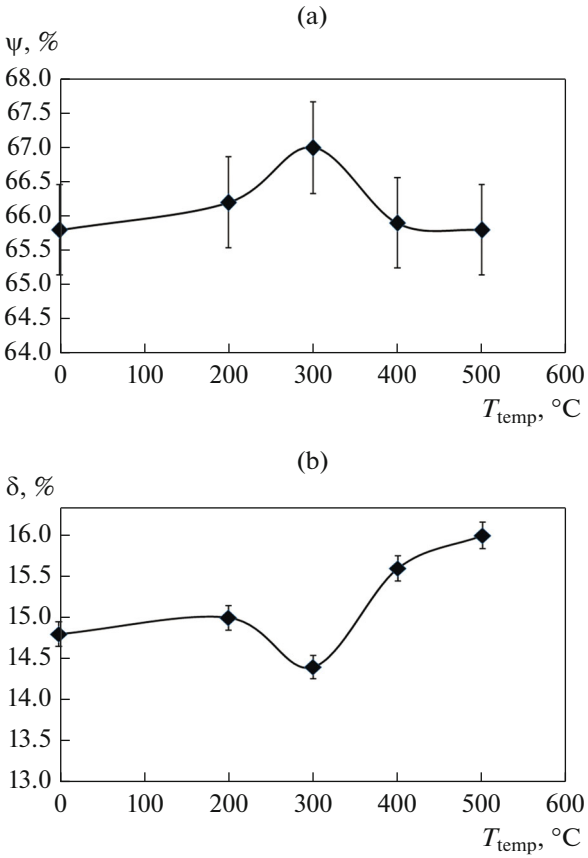

Fig. 4. Plasticity characteristics of the air-quenched steel 07Kh3GNMYuA, depending on the tempering temperature: (a) relative reduction ψ, %; and (b) relative elongation δ, %.

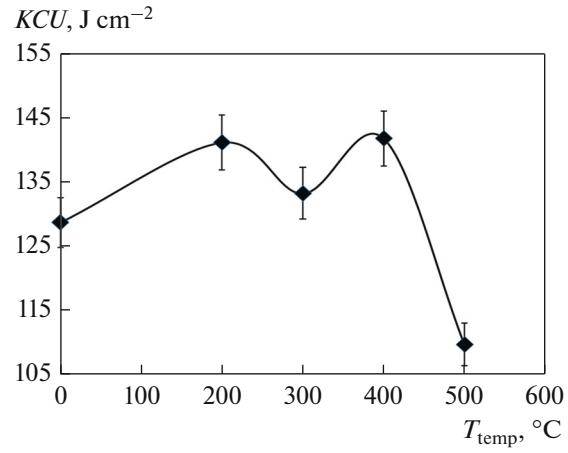

Fig. 5. Dependence of the impact toughness of the air-quenched 07Kh3GNMYuA steel on the tempering temperature.

U-shaped notch (Fig. 5). The changes in the impact toughness upon an increase in the tempering temperature are due to changes in the nature of fracture of the samples (Fig. 6).

After air-quenching and self-tempering, the fracture surface consists of regions of brittle fracture by cleavage, alternating with regions of dimpled gliding fracture (Fig. 6a). The fraction of dimpled (gliding) fracture does not exceed 10%. The clearly distinguishable river patterns (typical signs of fracture by cleavage) represent steps between the different local facets of the same common cleavage plane [9].

After the tempering at 200°C, the signs of brittle fracture disappear completely as a result of the relaxation of quenching stresses. Dimples (cells) of different sizes and dimples-cones (Fig. 6b) are observed on the surface of fracture. The fracture occurs via the mechanism of mergence of micropores. Second-phase particles are clearly visible at the bottom of the dimples, which are carbides no more than 1–2 μm in size. Accordingly, the impact toughness increases from 129 J/cm^2 in air-quenched steel to 141 J/cm^2 after tempering at 200°C

Approximately the same level of impact toughness is retained after the tempering at 400°C (142.0 J/cm^2). In the fracture, the fraction of dimples-cones increases significantly (Fig. 6d); the predominant mechanism of fracture is the formation and mergence of micropores. In the smooth regions, no river patterns are observed and these regions should not be considered as facets of cleavage or quasi-cleavage. Most likely, these are grain boundaries or regions of mergence of small cells into large dimples-cones. The fracture surface is characterized by a large number of second-phase particles (carbides).

The drastic reduction in the impact toughness of the steel 07Kh3GNMYuA upon the tempering at 300°C (133 J/cm^2) and 500°C (110 J/cm^2), which is associated with the phenomenon of tempering brittleness, leads to a change in the type of fracture. The dimpled ductile character of the fracture (gliding fracture) after the tempering at 200 and 400°C is replaced by a mixed character with signs of the intercrystalline type after the tempering at 300 and 500°C. This type of fracture is classified as being due to cleavage (in Figs. 6c, 6e, clearly distinguished river patterns are observed) and occurs over the internal volumes of the martensite laths and over the boundaries between them as a result of the formation of interlath carbides upon tempering.

It should be noted that after tempering at 300°C a small number of dimples and dimples–cones are retained on the fracture surface that are formed as a result of the mergence of micropores. The dispersity of the cells is higher than after tempering at 200°C, which is due to the fact that it is isolated dispersed carbide particles that serve as the regions of nucleation of microvoids. The fracture after tempering at 300°C is of mixed nature, where the fraction of the brittle component is significantly greater than that of the ductile component.

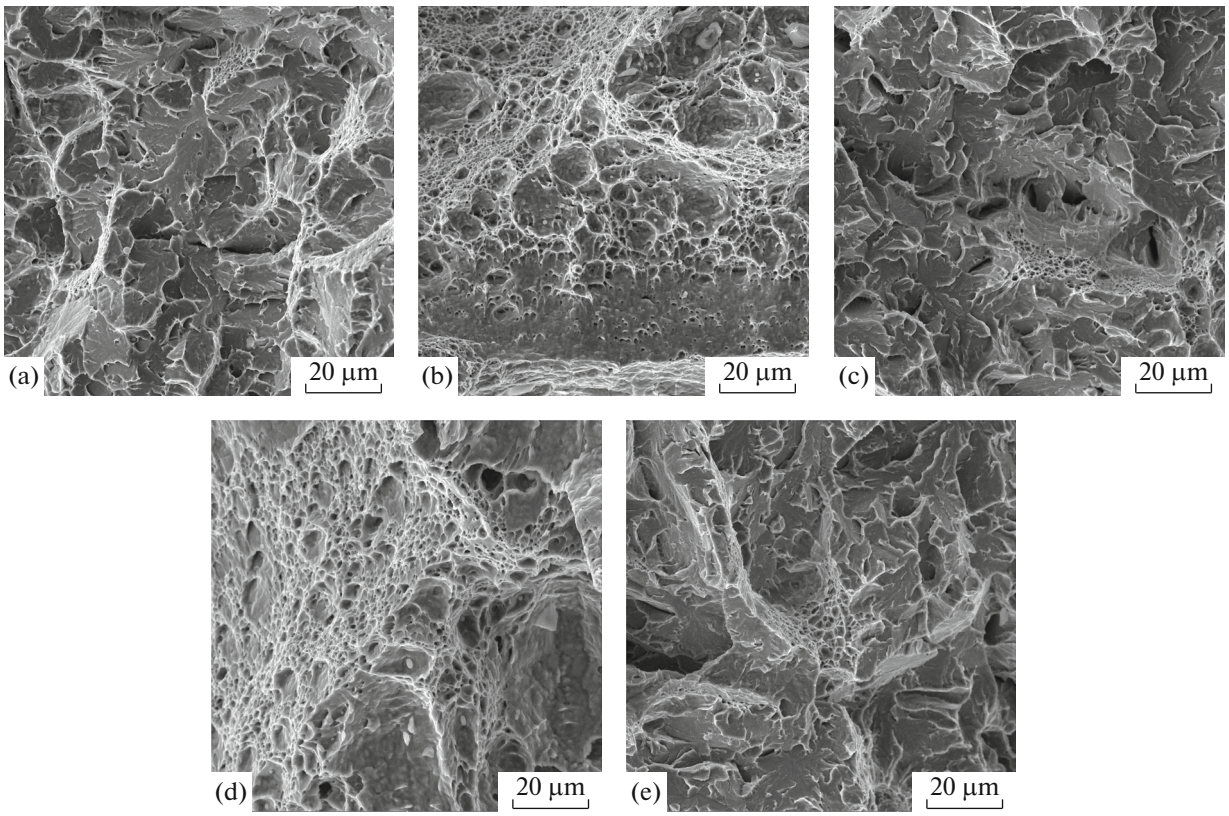

Fig. 6. Fracture surfaces of samples of steel 07Kh3GNMYuA: (a) after quenching; (b–e) after tempering at (b) 200, (c) 300, (d) 400, and (e) 500°C.

After tempering at 500°C, the intercrystalline fracture occurs via a catastrophic brittle splitting of grain boundaries because of their softening by carbide particles and segregates of non-metallic impurities, mainly, phosphorus-containing ones [10]. The inhomogeneity of the distribution of grain-boundary segregates leads to a mixed mechanism of fracture; as a result, in the case of the intercrystalline fracture regions of dimpled relief are observed. The preferred path of fracture along grain boundaries is not continuous, and in the fracture there are (in a small amount) fracture regions of cleavage kind present with a pronounced river-pattern structure.

Thus, the images of fractures show a clear connection between the nature of fracture and the mechanical characteristics of the 07Kh3GNMYuA steel, which depend primarily on the structural state of the steel created by heat treatment, on both micro- and submicro-levels.

The non-linear nature of the dependences of the mechanical characteristics on the tempering temperature should be taken into account upon the development of strengthening technologies for parts of machines and structures made of this steel.

CONCLUSIONS

(1) In the process of air-quenching in the steel 07Kh3GNMYuA, self-tempering processes are developed and a packet “structureless” martensite is formed alternating with ferrite regions. The processes of martensite decomposition that began during cooling in air continue in steel at subsequent temperings at 200, 300, 400, and 500°C with the formation of ferrite–carbide mixtures of different degrees of dispersity.

(2) The plasticity characteristics of the 07Kh3GNMYuA steel vary nonmonotonically depending on the tempering temperature. At the tempering temperatures of 300 and 500 °C, the impact toughness is reduced anomalously (by 6 and 23%, respectively). The relative elongation δ after tempering at 300°C decreases by 4%.

(3) Upon tempering at 200–400°C, an increase of the resistance to plastic deformation is observed in the steel: a monotonic increase occurs in the yield stress (by 11%). The further increase in the tempering temperature to 500°C leads to a decrease in the yield strength by 3%.

(4) The increase in the temperature of tempering is accompanied by a change in the nature of fracture of

the samples. If, after quenching and self-tempering, the fracture represents regions of brittle fracture by cleavage alternating with regions of dimpled ductile fracture, after tempering at 200 and 400°C the fracture occurs entirely via the mechanism of micropore mergence.

(5) After tempering at 300 and 500°C, the dimpled ductile nature of the fracture observed after tempering at 200 and 400°C is replaced by a brittle intercrystalline fracture, which is related to the phenomenon of temper brittleness. The data obtained using scanning electron microscopy are in good agreement with the results of mechanical tests.

(6) The non-linear nature of the dependences of mechanical characteristics on the tempering temperature should be taken into account upon the development of strengthening technologies for parts of machines and structures made of this steel with a yield strength of $\sigma_{0.2} = 830$ MPa.

FUNDING

The work was supported by a grant of the President of the Russian Federation for state support of young Russian scientists no. MK-6069.2018.8.

REFERENCES

1. L. M. Kleiner, *Structural High-Strength Low-Carbon Steels of Martensitic Class. A Tutorial* (Perm. Gos. Tekhn. Un-t, Perm, 2008) [in Russian].
2. L. M. Kleiner, *Novel Structural Materials: Low-Carbon Martensitic and Powder Steels*. Applied Metal Science. A Tutorial for High School Students (Perm. Gos. Tekhn. Un-t, Perm, 2004) [in Russian].
3. I. I. Novikov, *Metal Science. In 2 vols. Vol. 1 Heat Treatment. Alloys* (MISIS, Moscow, 2014) [in Russian].
4. L. M. Kleiner and Yu. N. Simonov, "Structure and properties of low-carbon martensitic alloys," Metalloved. Term. Obrab. Met., No. 8, 46–48 (1999).
5. L. M. Kleiner, Yu. N. Simonov, A. S. Ermolaev, and M. G. Zakirova, "Structure and properties of low-carbon martensitic steels, hardened from the intercritical temperature range," Konstr.Kompozits. Mater., No. 4, 172–177 (2006).
6. A. P. Gulyaev, *Physical Metallurgy*. 7th Ed. (Metallurgiya, Moscow, 2015) [in Russian].
7. M. V. Belous, V. T. Cherepnin, and M. V. Vasil'ev, *Transformation during Tempering of Steel* (Metallurgiya, Moscow, 1973) [in Russian].
8. R. A. Vorob'ev, V. N. Dubinskii, and V. V. Evstifeeva, "Comprehensive analysis of fractures, microstructure, and physical and mechanical properties for the evaluation of the crack resistance of medium-carbon Cr–Ni–Mo steel," Phys. Met. Metallogr. **118**, 1015–1021 (2017).
9. *Fractography and Atlas of Fractographs*, Ed. by H. E. Boyer and T. L. Call (ASM Metals Park, Ohio, 1974; Metallurgiya, Moscow, 1982).
10. L. M. Utevskii, E. E. Glikman, and G. S. Kark, "Reversible tempering brittleness of steel and iron alloys," (Metallurgiya, Moscow, 1987) [in Russian].

Translated by S. Gorin